CHAPTER IV
RESEARCH METHODOLOGY

Chapter IV describes the experimental method of the research, which investigates the dielectric properties of NiO-based ceramics. The NiO-based powders are synthesized by three different methods: a direct thermal decomposition method, a polymer pyrolysis method, and a PVA method. The crystal structure and microstructure as well as chemical compositions of the NiO-based powders and ceramics are characterized by X-ray diffraction, scanning electron microscopy, and energy dispersive X-ray spectroscopy techniques, respectively. The details about the dielectric and electrical measurement are also included in this chapter.

4.1 Powder and ceramic sample preparation

4.1.1 Synthesis of NiO-based powder and ceramic by polymer pyrolysis method

$Ni(NO_3)_2.6H_2O$ (99.9%, Kento chemical), $LiNO_3$ (98%, Panreac), titanium(diisopropoxide) bis(2,4-pentanedionate) 75wt% in 2-propanol ($C_{16}H_{28}O_6Ti$, Ti solution) (99%, Acros), $Fe(NO_3)_3{\cdot}9H_2O$ (99.9%, Kento chemical), $C_{10}H_{14}O_5V$ (99.0%, Acros), $(NH_4)_2S_2O_8$, and acrylic acid were employed as starting raw materials for the synthesis of (Li, Ti)-doped NiO, (Li, V)-doped NiO, and (Li, Fe)-doped NiO powders by the polymer pyrolysis method. The details about various chemical compositions of the $Li_xTi_yNi_{1-x-y}O$ (LTNO), $Li_xV_yNi_{1-x-y}O$ (LVNO), and $Li_xFe_yNi_{1-x-y}O$ (LFNO) ceramics sintered from the powders were summarized in Table 4.1. These NiO-based powders and ceramics were prepared by the following steps. First, stoichiometric amounts of the starting raw metallic materials, corresponding to a designed nominal composition of each NiO-based ceramic with different concentrations of the co-doping, were dissolved in 10 g of acrylic acid aqueous solution (acrylic acid: H_2O=70:30 wt %) under constant stirring and heating at 100 °C. Second, a small amount (0.5 g) of 5% $(NH_4)_2S_2O_8$ aqueous solution as the initiator was added into the mixed acrylic acid solution to promote the

polymerization. Then, the each gel precursor for various conditions was dried at 350 °C for 1 h. All of dried gels were ground and later calcined at 700-750 °C for 5 h in air. The obtained NiO-based powders were pressed into pellet of 9.5 mm in diameter and ~1–2 mm in thickness by a uniaxial pressing method at 200 MPa. Finally, these pellets were sintered at 1200-1280 °C for 4 h in air.

Throughout this thesis, X-ray diffraction (XRD) (Philips PW3040, The Netherlands) and scanning electron microscopy (SEM) (LEO 1450VP, UK) with energy dispersive X-ray spectrometer (EDS) were used to characterize the phase composition and microstructure as well as the chemical compositions of the NiO-based powders and ceramics, respectively. The XRD patterns were recorded within a 25^{o}-85^{o} angle range of 2θ ; the scan step was 0.02^{o}/s. For the dielectric measurement, the sintered NiO-based ceramic samples were polished and electroded by silver paint on both sides of the disk-shaped samples. The dielectric and electrical responses of the samples were measured using a Hewlett Packard 4194A impedance gain phase analyzer over wide range of frequency (10^{2}–10^{7} Hz) and temperature (from -60 to 150 °C) at the oscillation voltage of 1.0 V. Each measuring temperature was kept constant with an accuracy of ±1 °C. The details about each measuring technique will be described in this chapter. The flowchart diagram showing the overview of this sample preparation method and characterization is illustrated in figure 4.1.

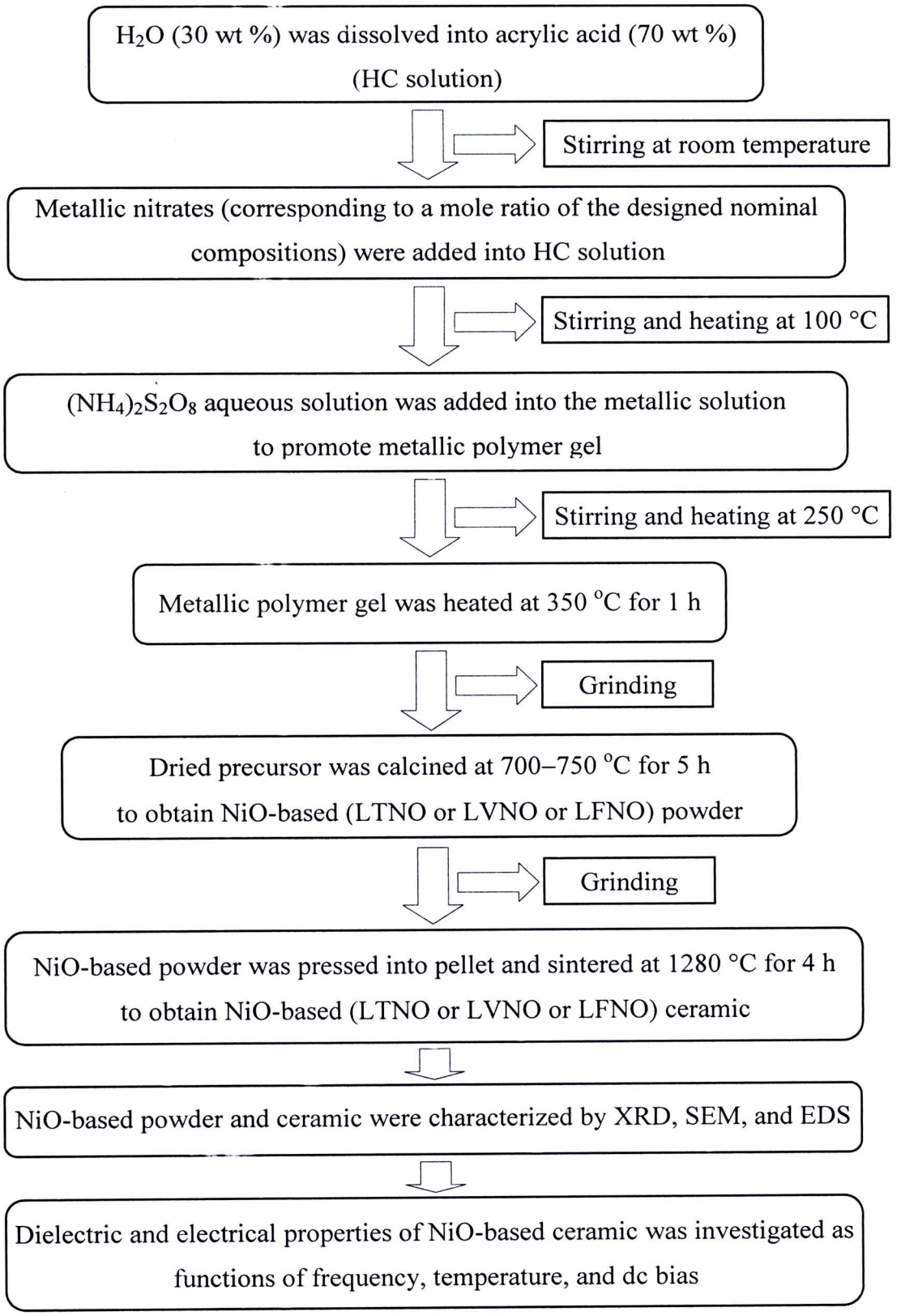

Figure 4.1 Diagram showing preparation and characterization of NiO-based powder and ceramic synthesized by the polymer pyrolysis method.

4.1.2 Synthesis of NiO-based powder and ceramic by direct thermal decomposition method

$(CH_3COO)_2Ni.4H_2O$ (99.0%, UNILAB), $C_2H_3LiO_2.2H_2O$ (≥97.0%, Fluka), and titanium(diisopropoxide) bis(2,4-pentanedionate) 75wt% in 2-propanol ($C_{16}H_{28}O_6Ti$, Ti solution) (99%, Acros), and $C_2H_5O_4Al$ (Sigma) were employed as starting raw materials for the synthesis of (Li, Ti)-doped NiO and (Li, Al)-doped NiO powders by the direct thermal decomposition method. The details about various chemical compositions of the $Li_xTi_yNi_{1-x-y}O$ (LTNO) and $Li_xAl_yNi_{1-x-y}O$ (LANO) ceramics sintered from the obtained powders were summarized in Table 4.1. These NiO-based powders and ceramics were prepared by the following steps. First, stoichiometric amounts of the starting raw metallic materials, corresponding to a designed nominal composition of each NiO-based ceramic with different concentrations of the co-doping, were dissolved into distilled water and mixed in alumina crucible using a magnetic stirrer. Then, each mixed solution was decomposed at a temperature of 650 °C for 10 h. The obtained NiO-based powders were pressed into pellets of 9.5 mm in diameter and ~1–2 mm in thickness by a uniaxial pressing method at 200 MPa. Finally, these pellets were sintered at 1200 to 1280 °C for 4 h in air. The flowchart diagram showing the overview of this sample preparation method and characterization is illustrated in figure 4.2.

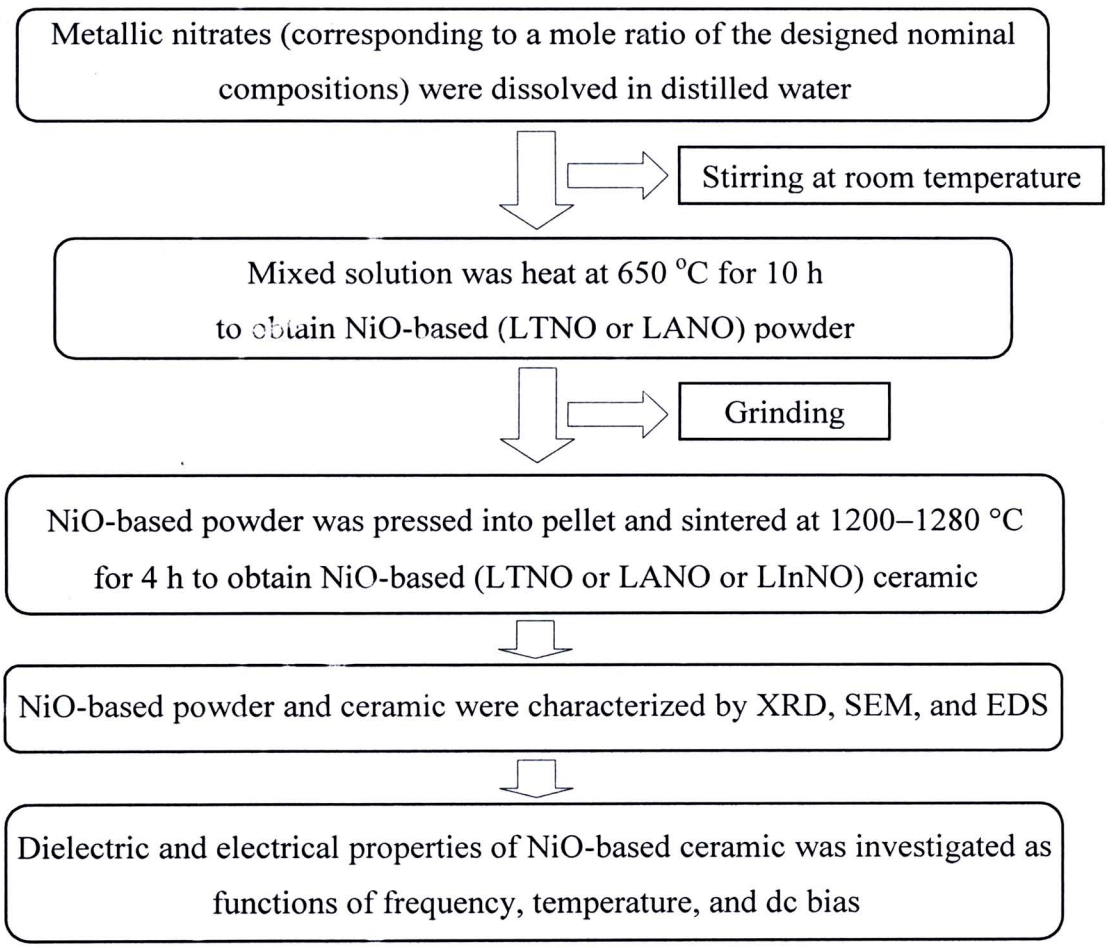

Figure 4.2 Diagram showing preparation and characterization of NiO-based powder and ceramic synthesized by the direct thermal decomposition method.

4.1.3 Synthesis of NiO-based powder and ceramic by PVA method

$Ni(NO_3)_2.6H_2O$ (99.9%, Kento chemical), $LiNO_3$ (98%, Panreac), titanium(diisopropoxide) bis(2,4-pentanedionate) 75wt% in 2-propanol ($C_{16}H_{28}O_6Ti$, Ti solution) (99%, Acros), $Fe(NO_3)_3{\cdot}9H_2O$ (99.9%, Kento chemical), citric acid ($C_6H_8O_7.H_2O$, 99%, BDH) and polyvinyl alcohol (PVA) ($[-CH_2CHOH-]_n$, M_n = 72 000, Fluka) were employed as starting raw materials for the synthesis of (Li, Ti)-doped NiO and (Li, Fe)-doped NiO powders by the PVA method. The (Li, Ti)-doped NiO powders with chemical formulas as $Li_xTi_yNi_{1-x-y}O$ (LTNO), where x=0.05, 0.10, 0.20 and y=0.02 and the $Li_xFe_yNi_{1-x-y}O$ powders were designed and prepared by the following steps. First, 5 g of citric acid was dissolved in 95 ml of distilled water (CA solution) with constant stirring using a magnetic stirrer at room temperature, and then 5 g of PVA was added into the CA solution (PVA solution) by stirring at 200 °C to obtain the polymer solution network. Second, stoichiometric amounts of $Ni(NO_3)_2.6H_2O$ and $LiNO_3$ were added into the PVA solution. Subsequently, Ti solution was slowly added into the mixed solution, followed by stirring and heating at 80 °C to form the transparent gel. Note that the ratio of CA solution: PVA: total amount of the precursors is about 100:5:10 wt%. Then, all of the gel precursors were dried at 100 °C overnight. To obtain the LTNO powders, these dried gels were ground and later calcined at 650 °C for 10 h in air. The LTNO powders were pressed into pellets 16 mm in diameter and ~1–2 mm in thickness by a uniaxial pressing method at 200 MPa. Finally, these pellets were sintered at 1250 °C for 5 h in air. The flowchart diagram showing the overview of this sample preparation method and characterization is illustrated in figure 4.3.

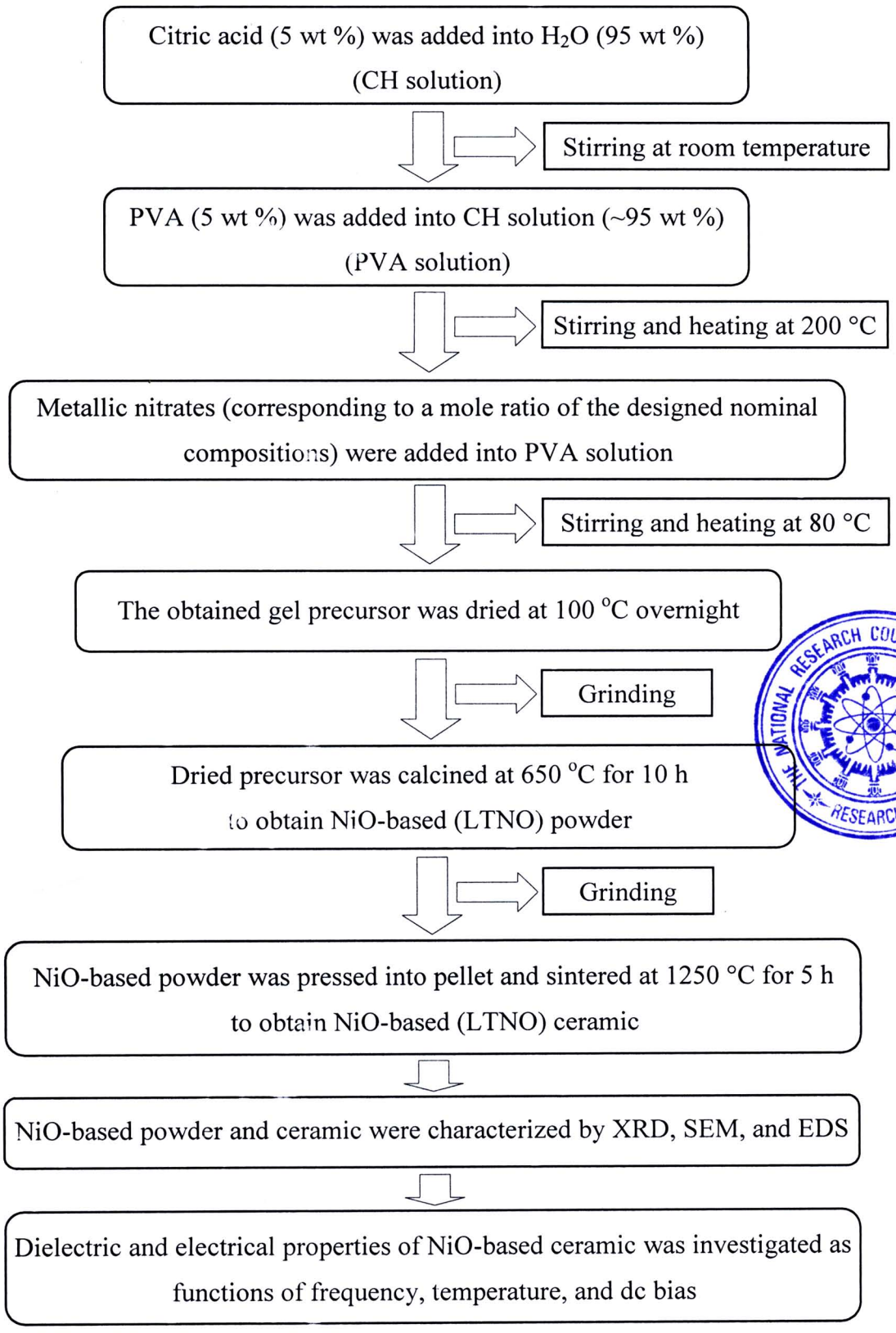

Figure 4.3 Diagram showing preparation and characterization of NiO-based powder and ceramic synthesized by the PVA method.

Table 4.1 List of starting raw metallic materials, NiO-based ceramic samples, and sintering condition for three preparation methods.

Metallic material	Nominal composition	Sintering condition
Polymer pyrolysis method		
$Ni(NO_3)_2.6H_2O$, $LiNO_3$, and $C_{16}H_{28}O_6Ti$	$Li_xTi_yNi_{1-x-y}O$ (LTNO)	Sintered at 1200, 1250, and 1280 °C for 4 h
	NiO	
	$Ti_{0.02}Ni_{0.98}O$	
	$Ti_{0.05}Ni_{0.95}O$	
	$Ti_{0.10}Ni_{0.90}O$	
	$Ti_{0.15}Ni_{0.85}O$	
	$Li_{0.05}Ti_{0.02}Ni_{0.93}O$	
	$Li_{0.05}Ti_{0.05}Ni_{0.90}O$	
	$Li_{0.05}Ti_{0.10}Ni_{0.85}O$	
	$Li_{0.05}Ti_{0.15}Ni_{0.80}O$	
	$Li_{0.02}Ti_{0.05}Ni_{0.93}O$	
	$Li_{0.10}Ti_{0.05}Ni_{0.85}O$	
	$Li_{0.10}Ti_{0.02}Ni_{0.88}O$	
	$Li_{0.02}Ni_{0.98}O$	
	$Li_{0.05}Ni_{0.95}O$	
	$Li_{0.10}Ni_{0.90}O$	
$Ni(NO_3)_2.6H_2O$, $LiNO_3$, and $Fe(NO_3)_3{\cdot}9H_2O$	$Li_xFe_yNi_{1-x-y}O$ (LFeNO)	Sintered at 1280 °C for 4 h
	$Fe_{0.05}Ni_{0.95}O$	
	$Li_{0.05}Fe_{0.02}Ni_{0.93}O$	
	$Li_{0.05}Fe_{0.05}Ni_{0.90}O$	
	$Li_{0.05}Fe_{0.10}Ni_{0.85}O$	
$Ni(NO_3)_2.6H_2O$, $LiNO_3$, and $C_{10}H_{14}O_5V$	$Li_xV_yNi_{1-x-y}O$ (LVNO)	Sintered at 1280 °C for 4 h
	$V_{0.05}Ni_{0.95}O$	
	$Li_{0.05}V_{0.02}Ni_{0.93}O$	
	$Li_{0.05}V_{0.05}Ni_{0.90}O$	

Table 4.1 List of starting raw metallic materials for each preparation of NiO-based ceramics system and of the ceramic samples with various nominal compositions and sintering conditions (Cont.).

Metallic material	Nominal composition	Sintering condition
	$Li_{0.05}V_{0.10}Ni_{0.85}O$	
	$Li_{0.02}V_{0.10}Ni_{0.88}O$	
Direct thermal decomposition method		
$(CH_3COO)_2Ni.4H_2O$, $C_2H_3LiO_2.2H_2O$, and $C_{16}H_{28}O_6Ti$	$Li_xTi_yNi_{1-x-y}O$ (LTNO)	Sintered at 1200 and 1280 °C for 4 h
	$Li_{0.05}Ti_{0.02}Ni_{0.93}O$	
	$Li_{0.05}Ti_{0.05}Ni_{0.90}O$	
	$Li_{0.08}Ti_{0.05}Ni_{0.87}O$	
$(CH_3COO)_2Ni.4H_2O$, $C_2H_3LiO_2.2H_2O$, and $C_2H_5O_4Al$	$Li_xAl_yNi_{1-x-y}O$ (LANO)	Sintered at 1280 °C for 4 h
	$Li_{0.05}Al_{0.04}Ni_{0.91}O$	
	$Li_{0.05}Al_{0.06}Ni_{0.89}O$	
	$Li_{0.05}Al_{0.10}Ni_{0.85}O$	
PVA-method		
$Ni(NO_3)_2.6H_2O$, $LiNO_3$, and $C_{16}H_{28}O_6Ti$	$Li_xTi_yNi_{1-x-y}O$ (LTNO)	Sintered at 1250 °C for 5 h
	$Li_{0.05}Ti_{0.02}Ni_{0.93}O$	
	$Li_{0.10}Ti_{0.02}Ni_{0.88}O$	
	$Li_{0.20}Ti_{0.02}Ni_{0.78}O$	
$Ni(NO_3)_2.6H_2O$, $LiNO_3$, and $Fe(NO_3)_3{\cdot}9H_2O$	$Li_xTi_yNi_{1-x-y}O$ (LTNO)	Sintered at 1250 °C for 5 h
	$Fe_{0.02}Ni_{0.98}O$	
	$Li_{0.02}Fe_{0.02}Ni_{0.96}$	
	$Li_{0.05}Fe_{0.02}Ni_{0.93}O$	
	$Li_{0.10}Fe_{0.02}Ni_{0.88}O$	
	$Li_{0.05}Fe_{0.05}Ni_{0.90}O$	
	$Li_{0.05}Fe_{0.10}Ni_{0.85}O$	

4.2 Powder and ceramic sample characterization

The crystal structure and microstructure of NiO-based powders and ceramics, prepared in this research, were characterized by XRD and SEM, respectively. The chemical compositions of the NiO-based ceramics and their distribution in the microstructure were investigated by SEM-EDS technique. The details about these measuring techniques are provided as follows.

4.2.1 X-ray diffraction (XRD)

In X-ray diffraction (XRD), a collimated beam of X-rays is incident on a specimen and is diffracted by the crystalline phases in the specimen according to Bragg's law

$$2d\sin\theta = n\lambda, \tag{4.1}$$

where d is the spacing between atomic planes in the crystal phase, n is an integer, λ is the wavelength of the X-ray radiation, and θ is the angle of incident beam. The intensity of the diffracted X-ray is measured as a function of the diffraction angle 2θ and the orientation of a specimen. The diffraction pattern can be used to identify the crystalline phases of the specimen and to measure its structural properties. Strain can also be measured accurately from the diffraction pattern; the size and orientation of crystallites (small crystalline regions) can be obtained as well. Furthermore, XRD can also determine concentration profiles, film thickness, and atomic arrangement in amorphous materials and multilayer; it can characterize defects, too. To obtain this structural and physical information from thin films, XRD instruments and techniques are designed to maximize the diffracted X-ray intensities, since the diffracting powder of the thin films is small (Loehman, Fitzpatrick, 1993).

In this thesis, the precise lattice parameter (a) of the crystal structure of NiO-based, which is a face-centered cubic structure, was calculated by using Cohen's least-squares method (Suryanarayana, Norton, 1998; Cullity, Stock, 2001),

$$\sum \alpha \sin^2\theta = A\sum \alpha^2 + C\sum \alpha\delta, \tag{4.2}$$

$$\sum \delta \sin^2 \theta = A \sum \alpha\delta + C \sum \delta^2 , \tag{4.3}$$

where,

$$A = \frac{\lambda^2}{4a^2}, \tag{4.4}$$

$$\alpha = h^2 + k^2 + l^2, \tag{4.5}$$

$$C = \frac{D}{10}, \tag{4.6}$$

$$D = -2K \cos^2 \theta , \tag{4.7}$$

$$\delta = 10 \sin^2 2\theta . \tag{4.8}$$

The experimental values of $\sin^2 \theta$, α, and δ can be substituted in to equations (4.2) and (4.3) for each of XRD peak. The value of A can be obtained by soling these two equations; as a result, the lattice parameter (a) can be calculated from equation (4.4). The constant C is related to the amount of systematic error involved and constant for any one sample.

4.2.2 Scanning electron microscopy (SEM)

The scanning electron microscopy is a technique that is used to image the sample surface by scanning it with a high-energy beam of electrons. The image of the sample surface can be obtained by interaction between the electrons and the atoms at or near the top surface of the sample producing signals that contain information about the surface morphologies of the sample and other properties such as composition and electrical conductivity. By using the signals to modulate the brightness of a cathode ray tube, which is raster scanned in synchronism with the electron beam, an image can be formed on the screen. Because of the very narrow electron beam, the obtained SEM images have a large depth of field yielding a

characteristic three-dimensional appearance useful for understanding the surface structure of a sample. Generally, the scanning electron microscope is often the first analytical instrument used when a 'quick look' at a material is required due to an optical microscope no longer provides adequate resolution (Loehman, Fitzpatrick, 1993).

According to the sample preparation required for this measuring technique, the sample must be electrically conductive, at least at the surface of the sample, and electrically grounded to prevent the accumulation of electrostatic charge at the surface. In the case of nonconductive ceramic samples, therefore, they are usually coated with an ultra-thin coating of electrically-conducting material. In this research, each NiO-based sample was firstly mounted rigidly on a specimen stub. Then, its surface was coated by gold to create the conductive surface of the NiO-based sample. Although some NiO-based samples were found to be conductive materials, these samples were also coated by gold because it can prevent the accumulation of static electric charge of the surface sample. Moreover, coating can also increase the signal and resolution. According to the SEM images, the mean grain size of each NiO-based ceramic sample can be estimated by direct measurement of the average diameter of each grain in the sample.

4.2.3 Energy dispersive x-ray spectroscopy (EDS)

When the atoms in a material are ionized by a high-energy radiation, they emit characteristic X-rays. EDS is an acronym describing a technique of X-ray spectroscopy that is based on the collection and energy dispersion of characteristic X-rays. An EDS system consists of a source of high-energy radiation (usually electrons) and signal processing electronics. X-rays are converted into signals which can be processed by the electronics into an X-ray energy histogram. This X-ray spectrum consists of a series of peak representative of the type and relative amount of each element in the sample. The number of counts in each peak may be further converted into elemental weight concentration either by comparison with standards or by standardless calculations (Loehman, Fitzpatrick, 1993).

In this research, the NiO-based ceramic samples were also characterized by the ESD technique in order to obtain the information about the distribution of the higher-valent doping ions on the microstructure. The surface and

fractured surface of the samples were characterized by this technique. As results, the chemical compositions at the grain and grain boundary regions can be determined.

4.3 Dielectric and electrical properties measurement

For the dielectric and related electrical measurement, the sintered NiO-based ceramic samples were polished by SiC paper to remove the outmost surface layer. Then, the samples were electroded by silver paint on both sides of the disk-shaped samples. The dielectric and electrical responses of the samples were measured using a Hewlett Packard 4194A impedance gain phase analyzer over wide range of frequency (10^2–10^7 Hz) and temperature (from -60 to 150 °C) at the oscillation voltage of 1.0 V. Each measuring temperature was kept constant with an accuracy of ±1 °C. The flowchart diagram showing the measuring dielectric parameters of the NiO-based ceramic samples was illustrated in figure 4.4. As shown in the flowchart diagram, the values of C_p and $\tan\delta$ at various frequencies and temperatures were obtained from the experimental measurement. The dielectric constant (ε') and dielectric loss (ε'') of the samples were calculated from the relations:

$$\varepsilon' = \frac{C_p d}{\varepsilon_0 A}, \tag{4.9}$$

$$\varepsilon'' = \varepsilon' \tan\delta, \tag{4.10}$$

where d is the sample thickness (m) and A is the area of electrode.

In this thesis, the electrical properties of the NiO-based ceramic samples were also investigated through the impedance (Z^*), modulus (M^*), and ac conductivity (σ_{ac}). These electrical parameters were calculated using the following equations:

$$\varepsilon^* = \varepsilon' - j\varepsilon'' = \frac{1}{j\omega C_0 Z^*}, \tag{4.11}$$

$$M^* = M' + jM'' = j\omega C_0 Z^*, \tag{4.12}$$

$$\sigma = \varepsilon_0 \omega \varepsilon'', \tag{4.13}$$

where ω is the angular frequency, $\omega = 2\pi f$ and $C_0 = \varepsilon_0 A / d$ is the empty cell capacitance.

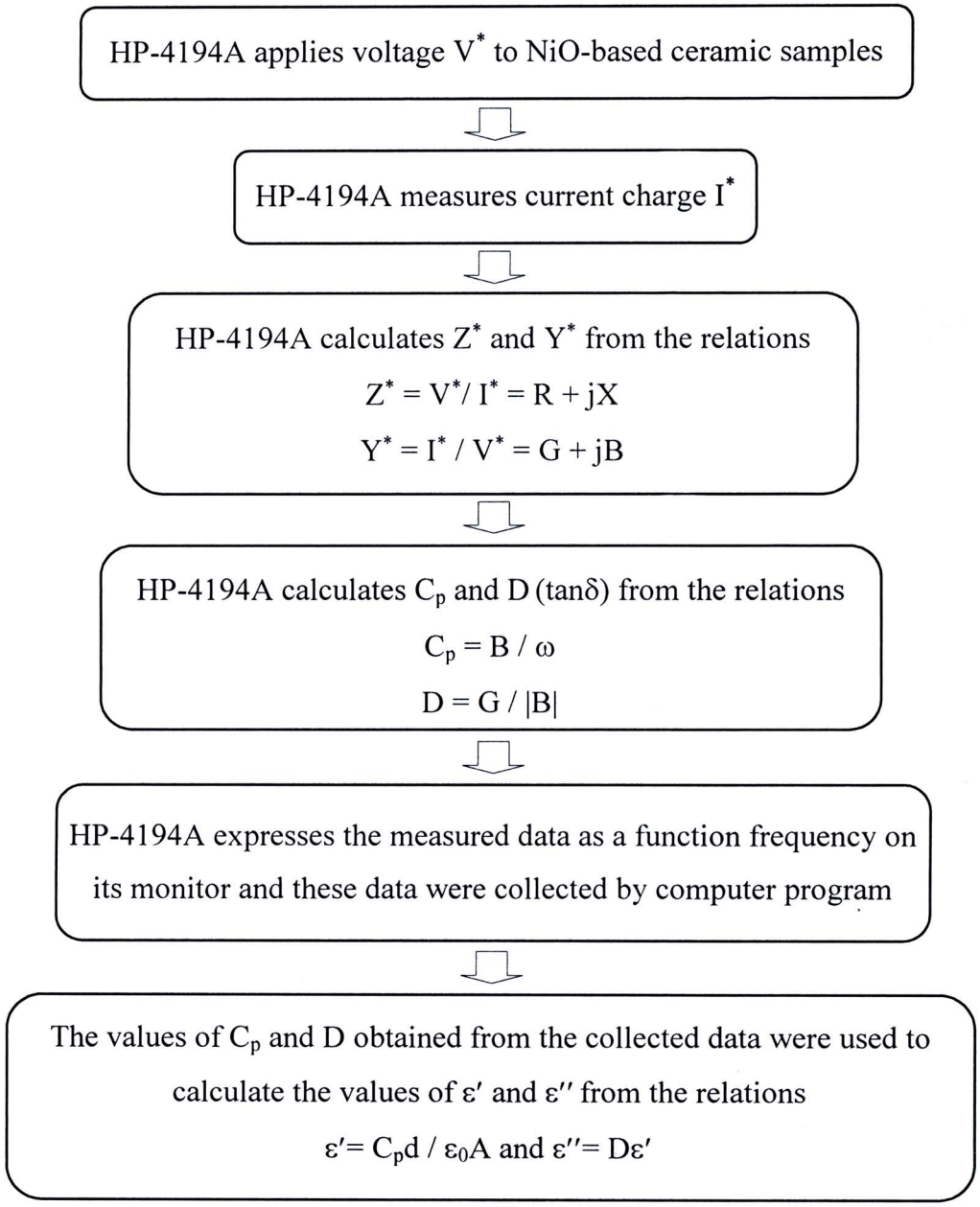

Figure 4.4 Diagram showing measuring dielectric parameters of the NiO-based ceramic samples using a Hewlett Packard 4194A impedance gain phase analyzer.